Encapsulation of Paclitaxel in Macromolecular Nanoshells

Alisar S. Zahr† and Michael V. Pishko*,‡

Departments of Chemical Engineering, Materials Science and Engineering, and Chemistry, The Pennsylvania State University, University Park, Pennsylvania 16802

Received February 13, 2007; Revised Manuscript Received April 10, 2007

An electrostatic layer-by-layer self-assembly technique was used to encapsulate solid core paclitaxel nanoparticles within a polymeric nanometer-scale shell. This approach provides a new strategy for the development of polymeric vehicles that control drug release and target diseased tissues and cells specific to the ailment, such as breast cancer. Core paclitaxel nanoparticles, 153 ± 28 nm in diameter, were prepared using a modified nanoprecipitation technique. A nanoshell composed of multilayered polyelectrolytes, poly(allylamine hydrochloride) and poly(styrene-4-sulfonate) was assembled stepwise onto core charged drug nanoparticles. In vitro studies were performed to determine the anticancer activity of paclitaxel core−shell nanoparticles. Paclitaxel core−shell nanoparticles induced cell cycle arrest in the G2/M phase after 24 and 48 h of incubation with a human breast carcinoma cell line, MCF-7. Changes in MCF-7 cell morphology, fragmentation of the nucleus, and loss of cell−cell contacts indicated that the cells responded to paclitaxel core nanoparticles upon treatment for 24 and 48 h. Cells arrested in G2/M phase illustrated abnormal microtubule and actin cytoskeleton morphology. The core−shell drug nanoparticles fabricated using this procedure provide a new approach in the delivery of paclitaxel devoid of Cremophor EL, a solvent that causes adverse side effects in patients undergoing chemotherapy for treatment of metastasized mammary cancers.

Introduction

Paclitaxel (Taxol, Bristol-Myers Squibb, New York, NY) is a clinically useful anti-neoplastic agent in the treatment of advanced human cancers including ovarian and breast cancer.[1−3] Paclitaxel inhibits mitosis in cells by binding to the β-subunit of tubulin, which promotes microtubule assembly and stabilization.[4−6] The biological activity of paclitaxel results in the inhibition of cell proliferation and induction of apoptosis at low drug concentrations (0.005−0.05 μM) and necrosis at high concentrations (5−50 μM).[7,8] The clinical success of Taxol is impeded by its low solubility in water (solubility of ∼0.6 mM)[9] as well as in many pharmaceutically acceptable solvents.[2,4] An adjuvant consisting of Cremophor EL (polyethoxylated castor oil) and dehydrated alcohol is used in the current clinical administration of paclitaxel and causes serious side effects including neurotoxicity, hypersensitivity reactions, and nephrotoxicity.[4,7] To overcome the problems caused by Cremophor EL, alternative approaches for packaging paclitaxel are currently under investigation and include cationic liposomes,[1] polymer micelles,[10] polymeric biodegradable nanoparticles,[2,3,9] and albumin-stabilized nanoparticles.[11] Encapsulation of paclitaxel within the aforementioned vehicles can promote an increase in bioavailability, protection of the drug during administration, controlled drug release, and reduction of systemic toxicity.[3,9,11]

Here we report the fabrication of core−shell drug nanoparticles of paclitaxel and their anti-tumor in vitro activity with a breast carcinoma cell line, MCF-7. The nanometer-thick shell is composed of a multilayer polymer film fabricated by a layer-by-layer (LbL) self-assembly method. Advantages for encapsulating solid core paclitaxel nanoparticles within a polymeric nanoshell include reducing the potential for burst drug release often found in emulsified biodegradable nanoparticles,[12] reducing the systemic toxicity of paclitaxel by confinement, providing a surface for chemical modification with targeting ligands[13] and the hydrophilic polymer poly(ethylene glycol) (PEG) for cancer cell or tissue selectivity and biocompatibility,[6,14] and enabling the suspension of the drug carrier in a buffered aqueous nontoxic solution for intravenous injection. The thickness of the shell, wettability, and swelling behavior can be controlled by varying experimental conditions such as pH, ionic strength, polymer functionality, and polymer concentration.[15, 16] Core−shell nanoparticles provide an alternative method for delivery of water-insoluble anti-neoplastic agents such as paclitaxel.

Materials and Methods

Materials. Poly(allylamine) hydrochloride (PAH, $M_w \approx 60\,000$ Da) was purchased from Polysciences, Inc., USA. Poly(styrene-4-sulfonate) (PSS, $M_w \approx 70\,000$ Da) was purchased from Aldrich Chemicals, USA. Paclitaxel from *Taxus brevifolia* was purchased from Sigma-Aldrich, USA. A succinimidyl ester of poly(ethylene glycol) propionic acid (mPEG-SPA, $M_w = 20\,000$ Da) was purchased from Nektar, USA. Potassium chloride was purchased from Fisher Scientific, USA. Acetone and methanol were purchased from Sigma Chemicals, USA. Dimethyl sulfoxide (DMSO) was purchased from Calbiochem, USA. Ultrapure water used for all experiments and cleaning steps was obtained from a Barnstead Nanopure Diamond RO system having a specific resistance of greater than 18 MΩ/cm. Polyelectrolyte solutions were prepared in a 30 mM KCl solution consisting of additional 0.15 M NaCl (pH 7.4). Phosphate-buffered saline solution (PBS, pH 7.4) consisted of 1.1 mM potassium phosphate monobasic, 3 mM sodium phosphate dibasic heptahydrate, and 0.15 M NaCl. For the covalent attachment of PEG to the nanoshell, a 0.1 M sodium bicarbonate buffer solution at pH 8.34 was used. Antibiotic−antimycotic was purchased from Sigma Chemicals, USA. Fetal bovine serum (FBS) was purchased from Hyclone, USA. Flasks for cell culture, T-75, 6- and 24-well plates were

* Author to whom correspondence should be addressed. E-mail: mpishko@engr.psu.edu.

† Department of Chemical Engineering.

‡ Departments of Chemical Engineering, Materials Science and Engineering, and Chemistry.

10.1021/bm070177m CCC: $37.00 © 2007 American Chemical Society
Published on Web 05/19/2007

Table 1. Experimental Conditions for Trials Performed To Fabricate Paclitaxel Solid Core Nanoparticles

trial no.	organic-to-aqueous ratio (v/v)	organic composition	homogenization speed (rpm)	size (nm) from SEM images
1	4:1	2 mg paclitaxel/acetone	6000	300 polydisperse
2	3:1	2 mg paclitaxel/acetone	6000	100 monodisperse
3	2:1	2 mg paclitaxel/methanol	6000	80 monodisperse

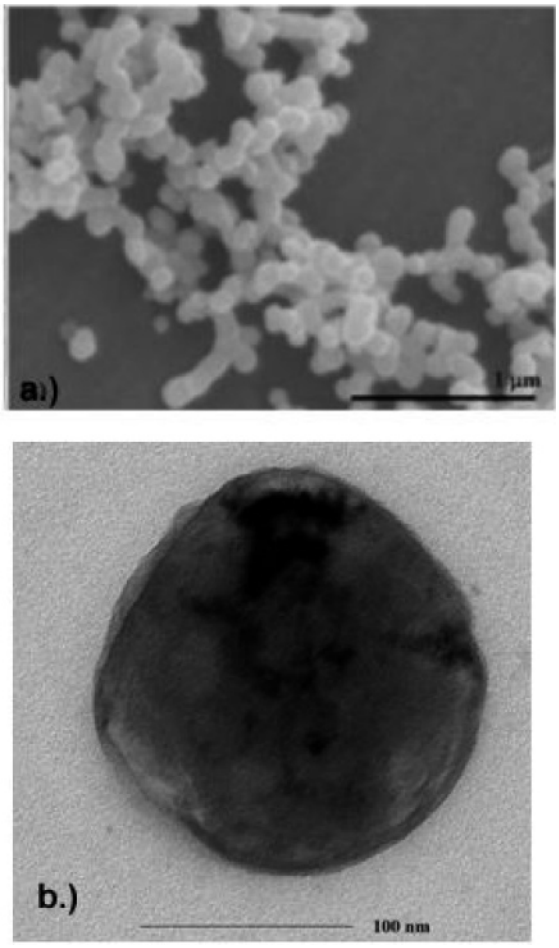

Figure 1. Images of paclitaxel core and core−shell drug nanoparticles. (a) SEM image of core drug nanoparticles prepared using high speed homogenization with an organic-to-aqueous ratio of 3:1, ×40 000 at 5.00 kV. (b) TEM image of core−shell drug nanoparticle encapsulated within a nanoshell composed of PAH/PSS/PAH, ×100 000.

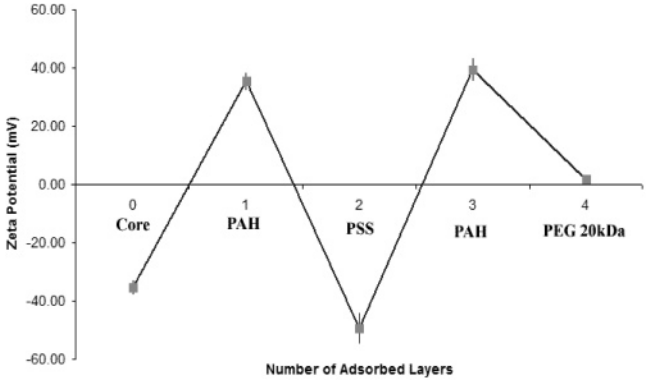

Figure 2. ζ-potential (mV) of core paclitaxel nanoparticles and each adsorbing polyelectrolyte layer. Each data point represents the mean ± standard deviation obtained from duplicates of four independent experiments. The 20 kDa PEG data point represents the mean ± standard deviation obtained from duplicates of three independent experiments.

purchased from VWR, USA. Centrifuge filters of sizes 0.2 and 0.45 μm were purchased Millipore, USA, and Pall Life Sciences, USA, respectively. Nalgene syringe filters were purchased from Nalge Nunc International, USA. An Eppendorf centrifuge 5810 was used for the centrifugation procedures.

Methods. *ζ-Potential Measurements.* The ζ-potential of each adsorbing layer was determined with a Brookhaven ZetaPALS instrument. Aqueous electrodes were used for these measurements. Samples were run at room temperature and dispersed in 30 mM KCl. The ζ-potential for one sample was calculated from 5 runs, and each run required 25 iterations.

Transmission Electron Microscopy. A JEOL JEM 1200 EXII transmission electron microscope was used to image the core−shell nanoparticles. Core−shell nanoparticles (in a solution of ethanol/water) were placed on copper grids for imaging. A high-resolution Tietz F224 camera was used to take digital images. All images were acquired at a tension of 80 kV and a current density of 20 pA/cm^2.

Scanning Electron Microscopy. Images of the solid core drug nanoparticles were obtained from a Hitachi S-3000H unit. Sample preparation included spraying a suspension of drug nanoparticles in 70% isopropanol/30% deionized water onto scanning electron microscopy (SEM) specimen holders. The sample was allowed to dry under ambient conditions for a day prior to imaging. Next, the sample was gold-sputtered for 30 s to minimize charging.

Particle Size Distributions. The particle size distributions of the centrifuge-filtered sample fractions were analyzed by a ZetaSizer Nano ZS. Material indexes of refraction for both polyelectrolytes were set to 1.46, and PBS solution was set to 1.33. A volume of 1.5 mL of the drug particle solution was pipetted into a disposable cuvette. Data were collected at room temperature.

Culture of MCF-7 Cells. Human epithelial breast cancer cells, MCF-7 (American Type Culture Collection, Rockville, MD, USA) were grown in minimum essential medium (American Type Culture Collection, Rockville, MD, USA) supplemented with 10% FBS, 1% streptomycin, and 0.01 mg/mL bovine insulin (Sigma-Aldrich, USA). The cells were grown in T-75 flasks to a density of 10^5 cells/mL and then subcultured into 6-well plates (1 mL of cells with 1 mL of medium) and incubated at 37 °C in an atmosphere containing 5% CO_2 for 24 h. For confocal image analysis, cells were plated onto circular glass cover slips (25 mm, VWR, USA) and grown 24 h prior to inoculation with core−shell nanoparticles. All experiments were performed in 10% serum.

Flow Cytometric Assay. Cell cycle analyses were performed on an XL-MCL flow cytometer (Beckman-Coulter, Miami Lakes, FL). Cells subcultured into 6-well plates were trypsinized and then fixed in 70% ethanol. The cells were then centrifuged, and the pellet was treated with 10 μL of RNase, DNase-free (10 mg/mL) (Roche Diagnostics, Inc., USA), and with 10 μL of propidium iodide (1 mg/mL). The cells were incubated in these solutions for 20 min at room temperature. Forward-scatter (FS) and side-scatter (SSC) dot plots gave the cellular physical properties of size and granularity. After 488 nm laser excitation, a 550 nm dichroic long-pass filter split the emission sending the green light to PMT1, which has an additional 525 nm bandpass filter, and the red light to PMT 3, which has an additional 610 nm bandpass filter. Propidium iodide positive cells were eliminated from the green distribution. Approximately 10 000 live cells were counted. DNA cell cycle analysis was collected using MultiFlow software.

Confocal Microscopy. Image analysis was performed on an Olympus FV300 laser scanning confocal microscope. Green fluorescence, Calcein

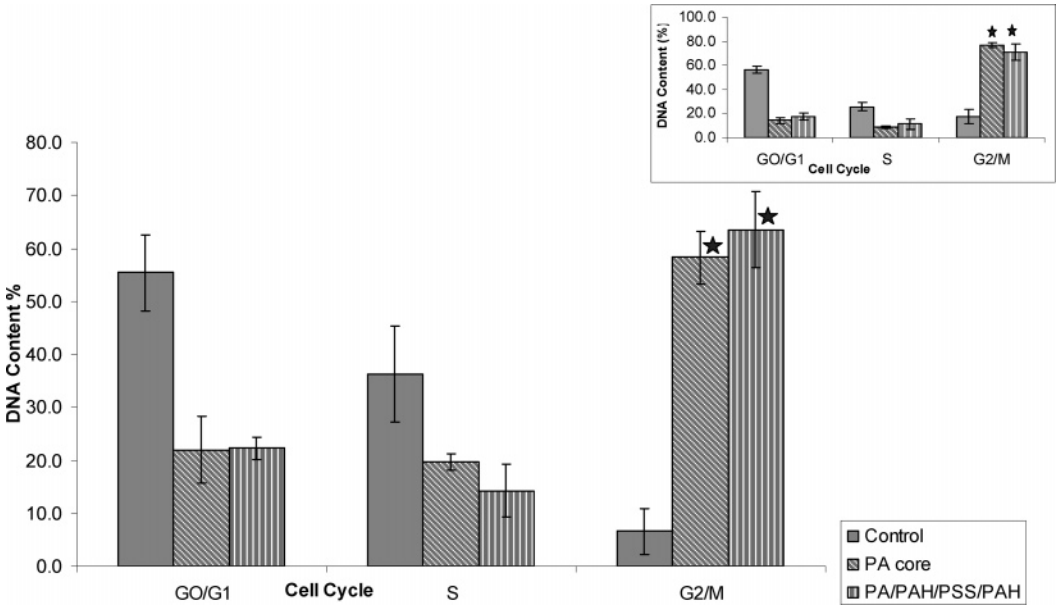

Figure 3. MCF-7 cells arrest in the G2/M phase following core paclitaxel nanoparticle and core−shell paclitaxel (PAH/PSS/PAH) treatment. Cells were treated with either 22 μg/mL of core or 22 μg/mL core−shell nanoparticles for 24 h. Inset: Results from a 48 h study performed with core and core−shell nanoparticles. Results represent the mean ± standard deviation from of 2−4 independent studies with 5−6 runs per experiment. Paclitaxel core and core−shell nanoparticles (as indicated by stars) were statistically significant compared to the negative control, which was the 100 μL of PBS.

AM (Molecular Probes, USA) was collected on channel 1 after 488 nm argon laser excitation. Phalloidin Alexa Fluor 568 (Molecular Probes, USA) used to stain the actin cytoskeleton was collected on channel 2 after 543 nm helium−neon laser excitation. Far red fluorescent DNA dye DRAQ5 (Biostatus Limited, U. K.) was used as a nuclear stain. A 560 nm dichroic filter split this emission light to the two photodetectors. The manufacturer's protocol was used for staining the F-actin cytoskeleton with Phalloidin Alexa Fluor 568, Molecular Probes, USA. Briefly, cells were fixed with a 3.7% formaldehyde solution in 0.1 M PBS for 10 min at room temperature and then washed with 0.1 M PBS. Next, 500 μL of a 1% Triton X-100 solution in PBS was added, and the cells were incubated in this solution for 5 min and subsequently washed two times with PBS. A 1% BSA blocking solution was added to each coverslip and left for 20 min. The working solution was prepared by diluting 5 μL of a 6.6 μM phalloidin methanol stock solution in 200 μL of PBS. After 20 min, 200 μL of the working solution was added to each coverslip and incubated with the cells at room temperature for 20 min. At the end of the incubation period, cells were washed two times with PBS with a final suspension in 1 mL of PBS. At this point 1 μL of DRAQ5 was added to each cover slip and incubated for 20 min at room temperature.

Microtubules were stained with Alexa-Fluor 488−Tubulin Tracker for live cell imaging (Molecular Probes, USA). A 1 mM stock solution of Tubulin Tracker was prepared by adding 71 μL of anhydrous DMSO to the lyophilized powder. Next, the 500 μM intermediate stock solution was prepared by adding 2 μL of the stock solution to 2 μL of a 20% Pluronic F-127 in DMSO. For final staining, 4 mL of media was added to the intermediate stock solution. For staining, 0.5 mL of the final stock solution was added to each coverslip and incubated at 37 °C, 5% CO_2 for 30 min. After 30 min, the cells were rinsed three times with PBS and viewed immediately with the confocal microscope.

Experimental Section

Core−shell drug nanoparticles were fabricated by a modified nanoprecipitation technique.[2] Nanoparticles of poly(lactic-*co*-glycolic acid) (PLGA) containing paclitaxel have been previously reported and prepared by oil-in-water emulsion,[4] spray drying,[17] and interfacial deposition[2] techniques. The nanoprecipitation method involves a one-step dispersion of an organic phase in the aqueous phase.[18] Unlike the previously reported nanoprecipitation fabrication of PLGA containing paclitaxel,[2] the method herein does not require the addition of a polymer within the organic phase. Briefly, an organic solution of paclitaxel (Sigma Aldrich, USA) in acetone was added to an aqueous solution containing a 2% (w/v) solution of GRAS surfactant calcium alginate (Sigma Aldrich, USA) under high magnetic stirring and low heat. The organic-to-aqueous solution ratio was maintained at 2:1. Solid drug nanoparticles were collected after 2 h, centrifuged, and resuspended in a PBS solution, pH 7.4. The morphology, size, and surface charge of the particles were characterized. Scanning electron microscopy was utilized to determine the morphology and size distribution of the solid core drug nanoparticles. Also, the particle size was confirmed with dynamic laser light scattering (ZetaSizer Nano ZS, refractive index, 1.60). The *z*-average was determined to be 153.3 ± 28.8 nm (polydispersity index, 0.22; $n = 4$). The size of the paclitaxel drug nanoparticles falls within the tumor pore cutoff size, which is important in the delivery of chemotherapeutic agents.[19] The surface charge of the core drug nanoparticles was determined by measuring the ζ-potential. The ζ-potential was determined to be -35 ± 2 mV ($n = 4$). This surface charge was due to the adsorption of surfactant to the surface of the particles. The surface charge of the drug nanoparticles was important because a charged substrate is required to utilize the LbL self-assembly method to construct a multilayer polymer shell.[20,21]

Results and Discussion

Experiments were performed to optimize the particle size, size distribution, and morphology of the core paclitaxel nanoparticles by varying the experimental conditions, which included the organic-to-aqueous volume ratio, the organic phase composition, and homogenization speed (rpm). Table 1 outlines the three experimental procedures performed to investigate the influence of the outlined parameters. The aqueous phase in all trials contained a 4% (w/v) solution of surfactant polyvinyl alcohol. SEM images illustrated that the experimental conditions affected the size, size distribution, and morphology of core paclitaxel nanoparticles. The core nanoparticles in trial 1 produced larger particles that were approximately 300 nm in diameter with a polydisperse distribution. Decreasing the

organic-to-aqueous ratio to 3:1 resulted in the formation of core particles that were approximately 100 nm in diameter with a homogeneous size distribution and a smooth/flat surface as shown in Figure 1a. Also, the composition of the organic phase had an influence on the size of the paclitaxel nanoparticles. Replacing acetone with methanol as the solvent in the organic phase decreased the size of the solid core particles to approximately 80 nm in diameter. Comparatively, a 2:1 ratio with acetone as the organic phase produced paclitaxel nanoparticles with a *z*-average of 166 ± 4 nm ($n = 2$) and monomodal in size. The results demonstrate that the size, size distribution, and morphology of the core paclitaxel particles can be controlled by varying the organic-to-aqueous volume ratio and organic composition. The results presented here are in agreement with literature results obtained by using the nanoprecipitation method to spontaneously form colloidal particles.[2,22]

Core paclitaxel nanoparticles were encapsulated within a polymeric nanosized shell by utilizing LbL self-assembly. LbL is a unique self-assembly procedure that can be used to prepare multilayer polymer films with controlled thickness on substrates through electrostatic interactions, hydrogen bonding, as well as hydrophobic interactions.[23−28] The principle behind this method of film preparation is the sequential adsorption of cationic and anionic polymers onto a charged substrate, and it was previously demonstrated that solid core nanoparticles of dexamethasone that had a negative charge can be encapsulated within a macromolecular nanoshell utilizing LbL assembly.[15,21] The polyelectrolyte pair poly(allylamine hydrochloride)/poly(styrene-4-sulfonate) (PAH/PSS) was chosen as a proof-of-concept to demonstrate the feasibility of using this method for fabricating a polymeric paclitaxel delivery vehicle without Cremophor EL as the solvent. Negatively charged core paclitaxel nanoparticles were encapsulated stepwise with PAH and PSS at a concentration of 20 mg/mL in a 30 mM KCl solution. After each adsorption period of 20 min, the particles were centrifuged (4000 rpm, 20 min) and resuspended in the 30 mM KCl. This cycle was performed three times. The ζ-potential was measured after each polyelectrolyte adsorption, and a reversal in charge demonstrated the successful stepwise encapsulation of core paclitaxel nanoparticles (Figure 2). Transmission electron microscopy (TEM) was used to visualize the polymeric nanoshell. Figure 1b clearly illustrates the nanosize of the shell with an approximate thickness of 10 nm with a composition of PAH/PSS/PAH.

Nanoparticles delivered by intravenous delivery are taken up by the liver, spleen, and other parts of the reticulo-endothelial system depending on size and surface characteristics.[6,29,30] To reduce the clearance of nanoparticles by macrophages, the drug delivery carrier is coated with hydrophilic polymers such as PEG.[31−33] The surface of the nanoshell was chemically modified with 20 kDa PEG by covalent attachment to the PAH adsorbed layer.[21] The ζ-potential of the nanoshell after chemical modification with 20 kDa PEG was determined to be 1.66 ± 1.04 mV ($n = 3$), Figure 2. In vitro uptake studies were previously performed with core−shell nanoparticles cultured with mouse macrophages, and results indicated that nanoshells modified with 20 kDa PEG or 2 kDa PEG reduced the percentage uptake compared to positively or negatively charged nanoshells.[34] Therefore, the neutral charge of the PEGylated core−shell paclitaxel nanoparticles should promote longer circulation times in vivo.

It has been recognized that paclitaxel-induced mitotic arrest results in apoptotic cell death in acute leukemia, prostate cancer, and breast cancer cells lines.[5,8] Apoptosis of paclitaxel-treated

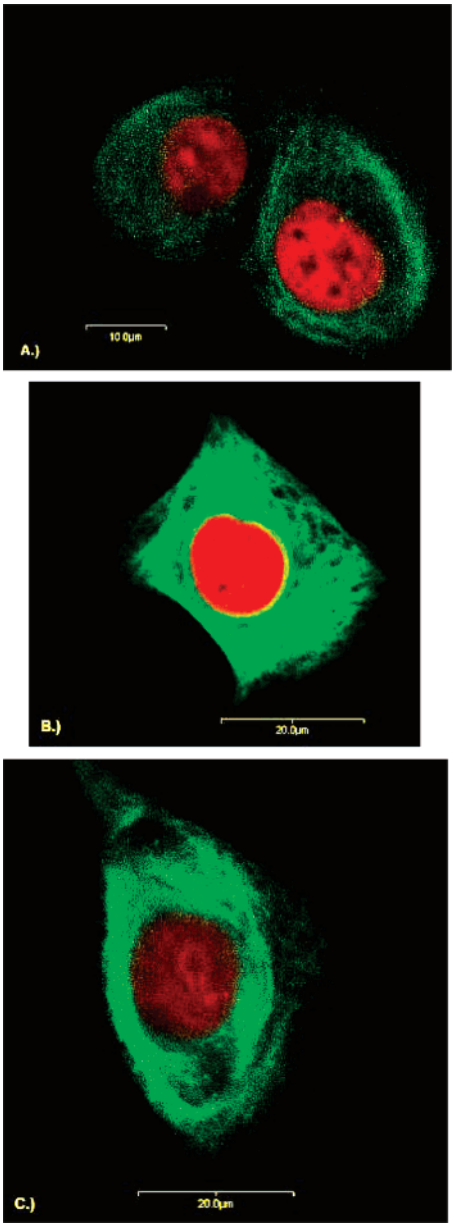

Figure 4. Effects of paclitaxel core−shell nanoparticles on microtubule structure and stability. MCF-7 cells grown on glass cover slips treated with (a) control or (b) core paclitaxel nanoparticles, 22 μg/mL for 24 h or (c) 48 h. Microtubules were stained with Tubulin Tracker Green, and nuclei were stained red with DRAQ5.

cells can occur at high concentrations and also upon prolonged treatment with low concentrations of the drug.[35] Lieu and co-workers found that low concentrations of paclitaxel induce apoptosis in human myeloid leukemia HL-60 cells in the G2/M phase and in the S phase.[36] Yeung and co-workers illustrated that Taxol treatment induced a biphasic decrease of viable cells in various breast cancer cell lines, apoptosis at low concentrations, and necrosis at high concentrations.[8] In opposition, Liao and co-workers revealed that in U937 cells paclitaxel induces apoptosis or a combination of apoptosis and necrosis depending on the cell cycle stage of the cell.[5] There seems to be a discrepancy in the literature concerning the mode of action of Taxol-treated leukemia, prostate, and breast cancer cells with low and high concentrations of Taxol.[5,8,37] In this study the goal was to demonstrate the in vitro anti-tumor activity of core and core−shell paclitaxel nanoparticles at a drug concentration of ~25 μg/mL. Due to a 10% loss from the fabrication procedure, the working concentration was 22 μg/mL rather than 25 μg/

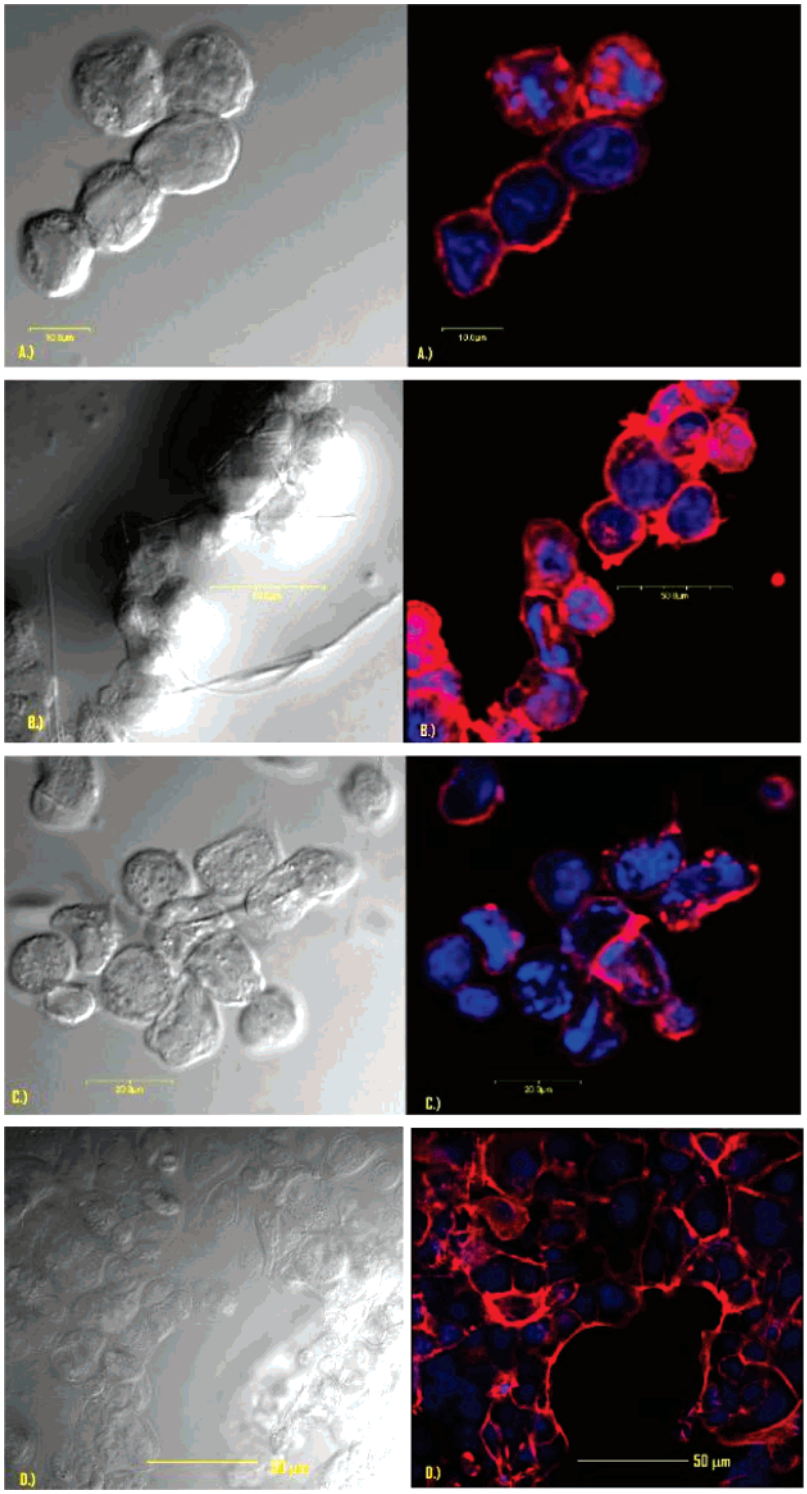

Figure 5. Changes in the actin cytoskeleton in MCF-7 cells treated with 22 μg/mL of solid core drug nanoparticles of paclitaxel for (a) 24 h, scale bar 10 μm, (b) 48 h, scale bar 50 μm, and (c) 72 h, scale bar 20 μm, and (d) control cells untreated for 24 h, scale bar 50 μm. F-actin was stained red with Phalloidin Alexa Fluor 568, and nuclei were stained blue with DRAQ5.

mL. This concentration was chosen because it corresponds to the plasma levels achievable in humans[38] and because Fonseca and co-workers demonstrated that at this concentration PLGA-loaded paclitaxel nanoparticles achieved the highest cytotoxic effect after 168 h of incubation with a small cell lung cancer line.[2]

Human breast cancer cells, MCF-7, were incubated with core and core−shell paclitaxel nanoparticles for 24 and 48 h. Flow cytometry was utilized to monitor the cell cycle progression of dose-treated MCF-7 cells, 22 μg/mL at $t = 0$. MCF-7 cells treated with both core and core−shell paclitaxel nanoparticles were blocked in the G2/M phase after 24 and 48 h of treatment (Figure 3). A two-tail Student *t*-test analysis was performed, and the results indicated that core and core−shell nanoparticles were statistically significant compared to the control at blocking MCF-7 cells at the G2/M phase. Also, the *t*-test analysis showed that both core and core−shell nanoparticles induced the same percentage of cell cycle inhibition at the G2/M phase. One concern in performing this study was that cellular toxicity may arise due to the PAH-coated, non-biocompatible nanoshell.

These results indicate that MCF-7 cells responded to the drug and not to the polymeric nanoshell.

The results in Figure 3 illustrate that the fabrication of paclitaxel solid drug nanoparticles and its encapsulation within a polymeric nanoshell did not weaken paclitaxel's mechanism of action. Upon prolonged treatment with paclitaxel core nanoparticles, MCF-7 cells were more sensitive to paclitaxel and were further accumulated at the G2/M phase, 76.7 ± 2% at 48 h compared to 58.3 ± 5% at 24 h (contrast to untreated cells which accumulated in the G0/G1 and S phase). The same trend was observed with core−shell paclitaxel nanoparticles; after 48 h 70.8 ± 7% of the MCF-7 cells were blocked at interphase in comparison to 63.5 ± 7% after 24 h. These results indicate that the encapsulation of solid drug nanoparticles within the polyelectrolyte nanoshell composed of PAH/PSS/PAH can control the dissolution and release of paclitaxel. The mechanism of drug release from the core−shell nanoparticles is hypothesized to occur by two routes. In the first route, core−shell nanoparticles carrying a positively charged surface can attach to the surface of the negatively charged membranes of the MCF-7 cells. As the drug is released from its encapsulation, a concentration gradient is generated that would favor drug influx into the cell.[2] The second route proposed by Fonseca and coworkers is the internalization of nanoparticles into the cell cytoplasm. This second route may not be dominant in this study because the internalization of the drug nanoparticles would require ligand−receptor complex and the surface of the nanoshell was not modified with targeting ligands. The results from the cell cycle analysis justify the importance of encapsulating this anti-tumor agent within a polymeric nanoshell and clearly demonstrate that paclitaxel activity is preserved within the polymeric nanoshell.

Microtubule stabilization upon treatment with paclitaxel core nanoparticles was visualized utilizing confocal microscopy. Live MCF-7 cells were treated with Tubulin Tracker Green and DRAQ5 to image cells treated with 22 μg/mL of paclitaxel core nanoparticles upon 24 and 48 h of incubation at 37 °C (Figure 4). Control MCF-7 cells exhibited a fine irregular meshwork of microtubules while dose-treated cells had apparent morphological differences. Loosely packed microtubule bundles were observed after 24 h of incubation with core nanoparticles. Also, as observed in Figure 4b, the microtubules were forming parallel alignments around the nucleus, which is indicative of microtubule stabilization.[39] After 48 h of incubation, the irregular meshwork had disappeared, and bundles of microtubules were formed. These results suggest that treatment with paclitaxel core nanoparticles was able to stabilize microtubules during cell cycle blockage at the G2/M phase. As discussed earlier microtubule dynamics play an imperative role in cell proliferation.[40]

The actin cytoskeleton plays an important role in tumor cells.[40] Changes involved in abnormal growth properties, such as the ability to adhere to tissue and the increased ability to metastasize, are mediated by the actin cytoskeleton. Anti-mitotic agents that affect the microtubule network reduce the level of tumor growth and migration, and these effects are hypothesized to occur via reorganization of the actin cytoskeleton.[41] If anti-mitotic agents induce cell death via apoptosis or necrosis, then changes in the microtubule network and in the actin filaments take place. As previously discussed, paclitaxel-treated cells have been shown to induce apoptosis after prolonged arrest in the G2/M phase.[8] Apoptosis is programmed cell death with distinct morphological features that include nuclear DNA fragmentation, membrane blebbing, loss of cell−cell contact, formation of apoptotic bodies, and actin granule formation near the plasma membrane.[42]

The results from microtubule staining suggested that MCF-7 cells were responding to treatment with paclitaxel nanoparticles, and the response of actin filaments to core dose-treated cells was studied. Paclitaxel nanoparticles were diluted to 22 μg/mL in cell culture medium and maintained at 4 °C for 5−6 days. After 6 days, confluent MCF-7 cells ($\times 10^5$ cells/coverslip) were treated with 2 mL of the paclitaxel-nanoparticle-treated medium and incubated at 37 °C in 5% CO_2 for 24, 48, and 72 h. Analysis of the actin cytoskeleton was completed using confocal microscopy. Figure 5 illustrates confocal images captured from dose-treated MCF-7 cells. Differential-interference-contrast images illustrate that the cells are rounded. In Figures 5b and 5c crystal-like structures are found attached to the cellular membrane, which is indicative of paclitaxel crystals. In all incubation periods, the nucleus of the cells contains fragmented DNA signifying cell death via apoptosis. An abnormal actin cytoskeleton is present after 24, 48, and 72 h of incubation with core nanoparticles. Actin granules located near the plasma membrane are more visible after 48 and 72 h of incubation. The actin filaments in 24 h treated cells show "diffusive fluorescence"[42] in the whole cell. Compared to the control MCF-7 cells, the cellular population of dose-treated cells did not exhibit a fine regular meshwork of short microfilaments (Figure 5).

Conclusion

Paclitaxel is one of the most effective anticancer agents in the treatment of metastatic breast carcinoma, but its therapeutic efficacy is limited because of the toxic solvents that are included in its formulation. Solid core paclitaxel nanoparticles, 153 ± 28 nm, were prepared using a modified nanoprecipitation technique and encapsulated within a polymeric nanoshell (~10 nm in thickness) assembled stepwise using the LbL assembly. Results collected by ζ-potential and TEM confirm the assembly of the nanoshell. Size and surface morphology of the core drug nanoparticles can be controlled by varying the organic-to-aqueous volume ratio and the choice of organic solvent. The organic-to-aqueous volume ratio has been identified in the literature as an important parameter for nanoparticle formation. The core−shell nanoparticles fabricated here provide a new opportunity for repackaging paclitaxel without the need for its dissolution in Cremophor EL/dehydrated alcohol.

In vitro studies with MCF-7 epithelial breast carcinoma cells illustrated that paclitaxel's therapeutic efficacy was retained upon its encapsulation within the multilayered polyelectrolyte nanoshell. DNA cell cycle analysis showed that paclitaxel core and core−shell nanoparticles were able to block MCF-7 cells at the G2/M phase. Furthermore, treatment with paclitaxel nanoparticles induced structurally morphological changes after 24 and 48 h of treatment of MCF-7 cells. Dose-treated cells, 22 μg/mL, displayed structural changes including a rounded plasma membrane with a loss of cell-to-cell contact and microtubule bundling and alignment after both 24 and 48 h. The intracellular concentration of paclitaxel was sufficient for microtubule stabilization and G2/M blockage but according to the findings from flow cytometry the concentration was too low to produce significant death via apoptosis or necrosis after 24 and 48 h of incubation. Dissolution of the hydrophobic core after 6 days and incubation with MCF-7 cells for 24 h induced cell apoptosis. Confocal images displayed MCF-7 cells with the actin granule formation near the plasma membrane and DNA fragmentation in the nucleus. The concentration of paclitaxel

in the medium was concentrated to provide such results. These findings provide important observations of the core−shell carrier described in this work; water-insoluble therapeutic agents can be fabricated into solid core drug nanoparticles and encapsulated within a polymeric nanoshell that retains the agent's efficacy in vitro.

Acknowledgment. This work was funded by the National Science Foundation (Grant No. NIRT BES-0210298). This project is funded, in part, under a grant with the Pennsylvania Department of Health using Tobacco Settlement Funds. The Department specifically disclaims responsibility for any analyses, interpretations, or conclusions. The authors appreciate the Center for Quantitative Cell Analysis for assistance in flow cytometry and confocal microscopy.

References and Notes

(1) Schmitt-Sody, M.; Strieth, S.; Krasnici, S.; Sauer, B.; Schulze, B.; Teifel, M.; Michaelis, U.; Naujoks, K.; Dellian, M. *Clin. Cancer Res.* **2003**, *9*, 2335−2341.
(2) Fonseca, C.; Simoes, S.; Gaspar, R. *J. Controlled Release* **2002**, *83*, 273−286.
(3) Gupte, A.; Ciftci, K. *Int. J. Pharm.* **2004**, *276*, 93−106.
(4) Feng, S.; Huang, G. *J. Controlled Release* **2001**, *71*, 53−69.
(5) Liao, P. C.; Lieu, C. H. *Life Sci.* **2005**, *76*, 1623−1639.
(6) Brannon-Peppas, L.; Blanchette, J. O. *Adv. Drug Delivery Rev.* **2004**, *56*, 1649−1659.
(7) Yeh, M.-K.; Coombes, A. G. A.; Jenkins, P. G.; Davis, S. S. *J. Controlled Release* **1995**, *33*, 437−445.
(8) Yeung, T. K.; Germond, C.; Chen, X.; Wang, Z. *Biochem. Biophys. Res. Commun.* **1999**, *263*, 398−404.
(9) Mitra, A.; Lin, S. *J. Pharm. Pharmacol.* **2003**, *55*, 895−902.
(10) Gao, A.; Lukyanov, A. N.; Singhal, A.; Torchilin, V. P. *Nano Lett.* **2002**, *2*, 979−982.
(11) Sparreboom, A.; Baker, S. D.; Verweij, J. *J. Clin. Oncol.* **2005**, *23*, 7765−7767.
(12) Shenoy, D. B.; Antipov, A. A.; Sukhorukov, G. B.; Mohwald, H. *Biomacromolecules* **2003**, *4*, 265−272.
(13) Sunderland, C. J.; Steiert, M.; Talmadge, J. E.; Derfus, A. M.; Barry, S. E. *Drug Dev. Res.* **2006**, *67*, 70−93.
(14) Moghimi, S. M.; Hunter, A. C. *Crit. Rev. Ther. Drug Carrier Syst.* **2001**, *18*, 527−550.
(15) Burke, M.; Langer, R.; Brem, H. In *Encyclopedia of Controlled Drug Delivery*; Mathiowitz, E., Ed.; Wiley: New York; Vol. 2, pp 184−191.
(16) Antipov, A. A.; Sukhorukov, G. B. *Adv. Colloid Interface Sci.* **2004**, *111*, 49−61.
(17) Mu, L.; Feng, S. S. *J. Controlled Release* **2001**, *76*, 239−254.
(18) Fessi, H.; Puisieux, F.; Devissaguet, J. P.; Ammoury, N.; Benita, S. *Int. J. Pharm.* **1989**, *55*, R1−R4.
(19) Hobbs, S. K.; Monsky, W. L.; Yuan, F.; Roberts, W. G.; Griffith, L.; Torchilin, V. P.; Jain, R. K. *Proc. Natl. Acad. Sci. U.S.A.* **1998**, *95*, 4607−4612.
(20) Decher, G. *Science* **1997**, *277*, 1232−1237.
(21) Zahr, A. S.; de Villiers, M.; Pishko, M. V. *Langmuir* **2005**, *21*, 403−410.
(22) Quintanar-Guerrero, D.; Allemann, E.; Fessi, H.; Doelker, E. *Drug. Dev. Ind. Pharm.* **1998**, *24*, 1113−1128.
(23) Decher, G. *Science* **1997**, *227*, 1232−1237.
(24) Caruso, F.; Mohwald, H. *J. Am. Chem. Soc.* **1999**, *121*, 6039−6046.
(25) Sukhorukov, G. B.; Donath, E.; Davis, S.; Lichtenfeld, H.; Caruso, F.; Popov, V. I.; Mohwald, H. *Polym. Adv. Technol.* **1998**, *9*, 759.
(26) Klitzing, R. v.; Wong, J. E.; Jaeger, W.; Steitz, R. *Curr. Opin. Colloid Interface Sci.* **2004**, *9*, 158−162.
(27) Lutkenhaus, J. L.; Hrabak, K. D.; McEnnis, K.; Hammond, P. T. *J. Am. Chem. Soc.* **2005**, *127*, 17228−17235.
(28) Sukhishvili, S. A. *Curr. Opin. Colloid Interface Sci.* **2005**, *10*, 37−44.
(29) Hans, M.; Lowman, A. M. *Curr. Opin. Solid State Mater. Sci.* **2002**, *6*, 319−327.
(30) Kingsley, J. D.; Dou, H.; Morehead, J.; Rabinow, B.; Gendelman, H. E.; Destache, C. J. *J. Neuroimmune Pharmcol.* **2006**, *1*, 340−350.
(31) Gref, R.; Minamitake, Y.; Peracchia, M. T.; Trubetskoy, V.; Torchilin, V.; Langer, R. *Science* **1994**, *263*, 1600−1603.
(32) Moghimi, S. M. *Biochim. Biophys. Acta* **2002**, *1590*, 131−139.
(33) Moghimi, S. M.; Hunter, A. C.; Murray, J. C. *FASEB J.* **2005**, *19*, 311−330.
(34) Zahr, A. S.; Davis, C. A.; Pishko, M. V. *Langmuir* **2006**, *22*, 8178−8185.
(35) Jordan, M. A.; Wilson, L. *Nat. Rev. Cancer* **2004**, *4*, 253−265.
(36) Lieu, C. H.; Chang, Y. N.; Lai, Y. K. *Biochem. Pharmacol.* **1997**, *53*, 1587−1596.
(37) Ferrari, M. *Nat. Rev. Cancer* **2005**, *5*, 161−172.
(38) Raymond, E.; Hanauske, A.; Faivre, S. *Anti-Cancer Drugs* **1997**, *8*, 379−385.
(39) Jordan, M. A.; Toso, R. J.; Thrower, D.; Wilson, L. *Proc. Natl. Acad. Sci. U.S.A.* **1993**, *90*, 9552−9556.
(40) Jordan, M. A.; Wilson, L. *Curr. Opin. Cell Biol.* **1998**, *10*, 123−130.
(41) Hayot, C.; Debeir, O.; Van Ham, P.; Van Damme, M.; Kiss, R.; Decaestecker, C. *Toxicol. Appl. Pharamcol.* **2006**, *211*, 30−40.
(42) Veselska, R.; Zitterbart, K.; Jelinkova, S.; Neradil, J.; Svoboda, A. *Oncol. Rep.* **2003**, *10*, 1049−1058.

BM070177M